

RSC Advances



This is an *Accepted Manuscript*, which has been through the Royal Society of Chemistry peer review process and has been accepted for publication.

Accepted Manuscripts are published online shortly after acceptance, before technical editing, formatting and proof reading. Using this free service, authors can make their results available to the community, in citable form, before we publish the edited article. This *Accepted Manuscript* will be replaced by the edited, formatted and paginated article as soon as this is available.

You can find more information about *Accepted Manuscripts* in the [Information for Authors](#).

Please note that technical editing may introduce minor changes to the text and/or graphics, which may alter content. The journal's standard [Terms & Conditions](#) and the [Ethical guidelines](#) still apply. In no event shall the Royal Society of Chemistry be held responsible for any errors or omissions in this *Accepted Manuscript* or any consequences arising from the use of any information it contains.

Magnetically deliverable calcium phosphate nanoparticles for localized gene expression

Cite this: DOI: 10.1039/x0xx00000x

Michela Puddu^a, Nicolas Broguiere^b, Dirk Mohn^{a,c}, Marcy Zenobi-Wong^b, Wendelin J. Stark^a and Robert N. Grass^{a*}

Received 00th January 2012,
Accepted 00th January 2012

DOI: 10.1039/x0xx00000x

www.rsc.org/

Iron oxide doped tricalcium phosphate ($\text{Fe}_2\text{O}_3@\text{TCP}$) nanoparticles were designed as transfection vehicles and prepared by flame spray synthesis. Both components are known to be non-toxic and biocompatible. Calcium phosphate (CaP) facilitates DNA entry into cells without the need for toxic cationic mediators, while magnetic iron oxide allows for particle localization at a target site. Flame spray synthesis ensures easy and low-cost nanoparticle production in a reproducible way. $\text{Fe}_2\text{O}_3@\text{TCP}$ nanoparticles, exhibiting DNA-binding capacity in the presence of CaCl_2 , were tested for transfection of a green fluorescent protein (GFP) encoding plasmid with Human Embryonic Kidney 293 (HEK 293) cells. Commercial magnetic agents, polyethylenimine (PEI) and standard calcium phosphate-mediated transfection were used for comparison. Transfection efficiency was estimated by GFP expression detected by fluorescence microscopy, while hoechst/ethidium homodimer-1 staining allowed the evaluation of method toxicity. We were able to efficiently transfect HEK 293 cells, and showed that $\text{Fe}_2\text{O}_3@\text{TCP}$ particles and bound DNA can be concentrated in specific sites in a culture plate through the application of a magnetic field gradient to achieve localized transfection. While the commercial magnetic controls strongly affected cell growth and morphology, $\text{Fe}_2\text{O}_3@\text{TCP}$ particles did not show marked toxicity and had only limited effects on cell proliferation. Overall performance in term of transfection efficiency, cell proliferation and viability, were comparable to that of CaP and PEI, which lack magnetic targeting capability. The newly synthesized $\text{Fe}_2\text{O}_3@\text{TCP}$ are, therefore, improved tools to deliver nucleic acid into cells and achieve spatial control of transfection.

Introduction

The process of introducing nucleic acids into cells is crucial for gene therapy, gene function and regulation studies, tissue engineering, as well as for protein manufacturing. The ideal transfection agent, besides giving high transfection efficiency, should be biocompatible and biodegradable, non-toxic to cells, non-immunogenic, and not affecting cell physiology. Additionally, it should be cost-effective, easy to prepare and apply, and be reproducible.

Viral vectors are the oldest and most efficient tools known to deliver genes. Despite ease and effectiveness of virus-mediated transfection, such vectors have shown to provoke an immune response.¹ Therefore, several non-viral vectors have been developed, that are less efficient than virus-based systems but exhibit enhanced biosafety.

Among the non-viral vectors, the most commonly-used systems are cationic polymer-based (e.g. polyethylenimine, PEI).²⁻⁵

Positively charged reagents interact electrostatically with negatively charged nucleic acids, forming complexes that are up-taken by cells via endocytosis. The technique is easy and inexpensive, but cationic components can be highly cytotoxic.⁶ Another simple and inexpensive option is calcium phosphate (CaP) mediated transfection.⁷⁻⁹ DNA is mixed with CaCl_2 and a saline/phosphate containing buffer to form precipitates carrying DNA into cells. DNA-calcium phosphate co-precipitates have been used for about 40 years to deliver nucleic acids. Biodegradability and biocompatibility of CaP,¹⁰⁻¹⁴ whose chemical composition mimicks that of natural bone mineral,^{10, 15} make CaP precipitates ideal transfection vehicles. However, transfection efficiency is inferior to other available non-viral agents. Additionally the method does not show enough reproducibility since size/shape and therefore transfection efficiency of the co-precipitates depend strongly on experimental factors (e.g. concentration, pH, precipitation time) and handling.^{9, 16} A combination of CaP and PEI transfection

techniques has also been developed to maximize transfection efficiency, leading though to reduced cell viability.¹⁴

A promising transfection technique is magnetically guided gene transfection or magnetofection.¹⁷⁻¹⁹ Nucleic acids are associated with magnetic particles (generally composed of iron oxide) and delivery is accomplished by the application of a magnetic field gradient. The method is universally suitable for viral and non-viral vector delivery and highly efficient. Most of the commercial magnetic particles are modified with cationic molecules able to complexate DNA. Magnetofection promises to solve fundamental problems associated with *in vivo* gene therapy, *i.e.* low vector availability at the target site, side effects related to high vector doses and vector distribution in non-targeted tissues. The magnetic particles together with the associated vectors can be delivered and retained by magnetic means at the disease site after injection, allowing reduction of vector doses and minimizing gene vector spreading throughout the body. However, biocompatibility in magnetofection can be compromised due to the cytotoxic nature of cationic species often used to mediate DNA binding to the particles.

Nowadays spatial control of gene delivery and expression in specific areas plays an important role not only in gene therapy, but also in synthetic biology.²⁰ By creating spatial patterns of gene expression in a cell culture one could recreate the complex architecture of tissues and organs.^{20, 21} Additionally, one could engineer artificial gene circuits mimicking natural networks to gain basic biological understanding of cellular processes or for practical applications.^{20, 22} Localized gene expression has been achieved using a robotic microarrayer to deposit gelatin-plasmid solutions,²³ near infrared irradiation of gold nanorods-green fluorescent protein gene conjugates,²⁴ lipoplex deposition using microfluidic devices,²¹ and lyophilization of adenovirus.²⁵ Above all, gene expression localization using magnetic particles represent an easy and precise way to define transfection patterns.^{20, 26}

In this study, we designed and produced a novel, polycation-free, CaP-based magnetic transfection agent which combines the above described advantages of standard CaP and magnetic beads mediated transfection, overcoming at the same time the obstacles presented by the two technologies. We produced a composite nanopowder made of iron oxide and tricalcium phosphate by flame spray synthesis. The material was characterized and tested as transfection mediator with HEK 293 cells to present its effectiveness.

Experimental section

Nanoparticle production

Iron oxide doped tricalcium phosphate nanoparticles ($\text{Fe}_2\text{O}_3@\text{TCP}$) were produced by flame spray synthesis.^{27, 28} Calcium-2-ethylhexanoate (superconductor grade, ABCR) and tributylphosphate (98%, Aldrich) were used as calcium and phosphor precursors, respectively. Iron precursor was prepared according to a previously described procedure.²⁹ The liquid

mixture with a Ca/P molar ratio of 1.5 and a final Fe_2O_3 content of 33 wt% was obtained by mixing the corresponding amounts. All precursors were diluted with xylene to a final metal concentration of 0.8 mol/L. The precursor solutions were fed through a capillary into a burning methane (1.13 L/min, Pan Gas, Switzerland)/oxygen (2.4 L/min, Pan Gas) supporting flame using a gear-ring pump (HNP Mikrosysteme, Germany) adjusted to a rate of 5 mL/min. Oxygen (5 L/min, Pan Gas) was used to disperse the liquid leaving the capillary. Produced nanoparticles were collected on metal filters (G. Bopp & Co AG, Switzerland) with the aid of a vacuum pump. A detailed description of the set-up can be found in.²⁷

Plasmid preparation

pAcGFP1-Endo plasmid (Clontech) was kindly provided by Prof. Dr. Wilfried Weber (Institute of Biology II/BIOSS Center for Biological Signalling Studies, Albert-Ludwigs-Universität Freiburg, Germany). The plasmid (5356 bp), which encodes the green fluorescent protein (GFP), was propagated in chemically competent *E. coli* (see Supplementary Information) and purified using the Qiagen Plasmid Midi kit. Obtained pDNA was diluted to a concentration of 0.6 $\mu\text{g}/\text{mL}$ and stored at -20°C .

Cell culture

HEK 293 for transfection experiments were grown in Dulbecco's modified Eagle's medium (DMEM, Invitrogen no. 41966) supplemented with 10% fetal bovine serum (FBS, Gibco) and 1% Penicillin/Streptomycin (Gibco). Cells were grown at 37°C and 5% CO_2 , and subcultivated according to standard cell culture protocols.

Transfection of mammalian cells

One day before transfection, cells were seeded in a 96-well plate (at a density in the range 312-937 cells/ mm^2) and cultivated in 100 μL media per well. Commercial transfection agents PolyMAG (Chemicell, Germany) and NeuroMag (OZ Biosciences, France), as well as traditional CaP and PEI transfection were used for comparison to the developed material. For each protocol, 0.4 μg pDNA per 96-well was used.

Transfection with PolyMAG (Chemicell, Germany) and NeuroMag (OZ Biosciences, France) was carried out according to the manufacturer's guidelines. 0.4 μg pDNA was dissolved in 19 μL serum-free media and mixed with the transfection reagent. For Polymag a ratio of 1 μL reagent/ μg pDNA was used, while for NeuroMag a ratio of 3.5 μL reagent / μg DNA was used. The mixture was left to stand 15 min at room temperature to allow for complexation. Then 80 μL of medium supplemented with serum was added.

To perform standard transfection with CaP, DNA was mixed with 4.4 μL of 2 M CaCl_2 solution and diluted with sterile ultra-pure water (SIMSV0000-Simplicity UV, Millipore) to a final volume of 35 μL . The prepared CaCl_2 -DNA solution was briefly vortexed and then added dropwise to 35 μL of HEPES buffered saline (BioUltra, 2X concentrate, Sigma Aldrich),

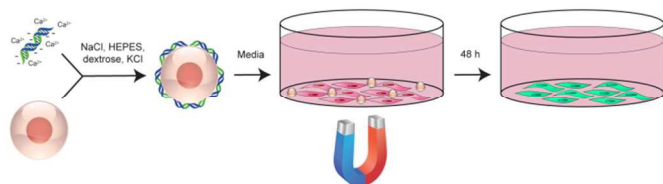


Fig. 1 Scheme of magnetic assisted cell transfection using $\text{Fe}_2\text{O}_3@\text{TCP}$ particles.

while vortexing. The suspension of CaP-DNA coprecipitates was incubated at room temperature for 15 min before adding 280 μL of media supplemented with serum. The prepared mixture was enough to transfect 3 wells (100 μL per 96-well).

Transfection with PEI was accomplished by mixing pDNA with PEI (branched, $M_n \sim 10000$, Sigma Aldrich) at a nitrogen/phosphate (N/P) molar ratio of 10 in serum free media (20 μL per well). The mixture was incubated for 15 min at room temperature before adding media supplemented with serum (80 μL per well).

The $\text{Fe}_2\text{O}_3@\text{TCP}$ powder was sterilized by heating at 200°C for 30 min. A fresh particle suspension was prepared each time before performing transfection experiments. Nanoparticles were dispersed in sterile ultra-pure water at a concentration of 1 mg/mL and sonicated at 200 W for 20 min. The following buffer was prepared in ultra-pure water: 16 g/L sodium chloride (NaCl for analysis EMSURE® ACS, ISO, Reag. Ph Eur.), 10 g/L HEPES ($\geq 99.5\%$ Sigma), 2 g/L D-(+)-glucose ($\geq 99.5\%$ Sigma) and 0.74 g/L KCl (Sigma Aldrich), with pH adjusted to ~ 7.5 . The overall transfection procedure is illustrated in Fig. 1. To prepare the transfection mixture for a well, 0.4 μg pDNA was mixed with 2 M CaCl_2 to achieve the desired molarity (in the range 62.5-100 mM) in the mixture and with the prepared buffer to a final volume of 20 μL . The CaCl_2 -DNA solution was briefly vortexed before adding the required volume (2 to 6 μL reagent / μg DNA) of particle suspension. The transfection mixture was vortexed again and left to stand for 15 min at room temperature. 80 μL of medium supplemented with serum was then added.

The transfection volume (100 μL per 96-well), was then added to the cells. A magnetic field (MagnetoFACTOR-96 plate, Chemicell, Germany) was applied for 30 min to PolyMAG, NeuroMag as well as to $\text{Fe}_2\text{O}_3@\text{TCP}$ nanoparticles, while incubating at 37°C and 5% CO_2 .

After 48 h, live/dead assay and transfection visualization/quantification were performed by fluorescence microscopy (see Supplementary Information). Transfection efficiencies are given as ratio of cells expressing GFP to the total number of cells. Viability data are provided as ratio of live cells to the total number of cells. Proliferation data are given as ratio of average number of cells in a sample to the average number of cells in the untreated control. Quality factors (QFs) are calculated as product of transfection efficiency, proliferation rate and viability. By definition the QF is zero for the untreated control, and 1 in the ideal case (*i.e.* transfection efficiency = proliferation rate = viability = 100%).

Localization of gene expression

One day before transfection the cells were seeded in a 55 mm diameter Petri dish with 4 mL of media, at a density of 312 cells/ mm^2 . Transfection mixture was prepared as described in the previous section by mixing DNA (8 μg) with 2 M CaCl_2 to achieve a CaCl_2 concentration of 100 mM in the transfection mixture volume (800 μL), saline buffer and particles (32 μL). The mixture was then diluted with media up to 4 mL. The Petri dish was placed over the MagnetoFACTOR-96 array. The transfection mixture was pipetted onto the cells overlaying the magnet positions. Cells were then incubated for 48 h onto the magnets.

Results and discussion

We engineered and synthesized a new transfection composite material. Our idea was to produce non-toxic magnetic particles with a surface able to bind DNA and to deliver it inside cells. Iron oxide, widely used in magnetofection and for various biomedical applications, was the obvious choice of magnetic material. An outer biodegradable calcium phosphate layer was highly preferred to iron oxide surface modification with generally more efficient but cytotoxic polycations. Because of their biocompatibility and biodegradability,³⁰⁻³³ iron oxide nanoparticles are the only metal oxide particle clinically approved (*e.g.* Feridex, a MRI contrast agent), and used as food additives (iron oxide pigment = E172). CaP high biocompatibility and easy integration in the body,¹⁰⁻¹⁴ where it is present in solid form or as calcium and phosphate ions,^{10, 14} has determined its Food and Drug Administration approval as nutrient and its use as bone-substitute in clinical treatments.¹⁰ CaP ceramic-iron oxide nanoparticle composites have been previously tested as potential bone replacement and proved to possess good biocompatibility and ability to promote cell proliferation *in vitro*.³⁴ An earlier attempt to produce magnetic CaP nanoparticles in a multi-step synthesis, comprising biomineralization of CaP on PEI-coated magnetic beads, has also been made.³⁵ The presence of the polycation though did not eliminate the potential toxicity of the formulation.

Flame spray synthesis was used to produce the designed magnetic particles, possessing an iron oxide core surrounded by a TCP matrix. It has been previously shown that the technology is capable of producing multi-component nanoparticles in a single step,^{36, 37} as here in the case of $\text{Fe}_2\text{O}_3@\text{TCP}$ nanocomposites. Additionally, flame spray technology enables large-scale production of nanoparticles with reproducible size distribution and at low cost.³⁸⁻⁴⁰ While CaP co-precipitates need to be prepared before performing each experiment, $\text{Fe}_2\text{O}_3@\text{TCP}$ powder can be stored in dry state, reducing the experimental variations and facilitating the handling.

The newly synthesized particles were fully characterized (see Electronic Supplementary Information for characterization methods). Brunauer-Emmett-Teller (BET) measurements of the nanoparticles gave a specific surface area of 68 m^2/g , which corresponds to a primary particle diameter of 25 nm,

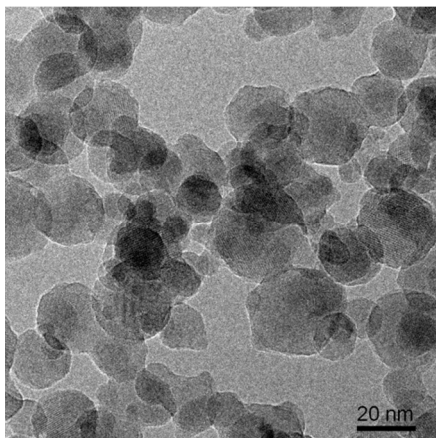


Fig. 2 TEM micrograph of Fe_2O_3 @TCP nanoparticles prepared by flame spray synthesis.

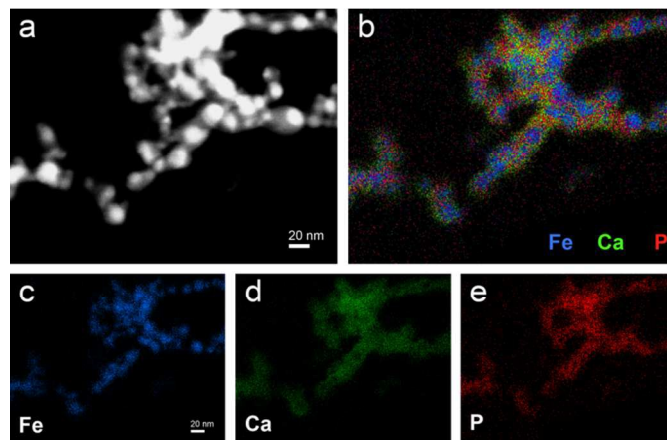


Fig. 3 (a) STEM image of Fe_2O_3 @TCP nanoparticles and corresponding elemental mapping of Fe, Ca, and P merged (b) and of the single elements (c-e).

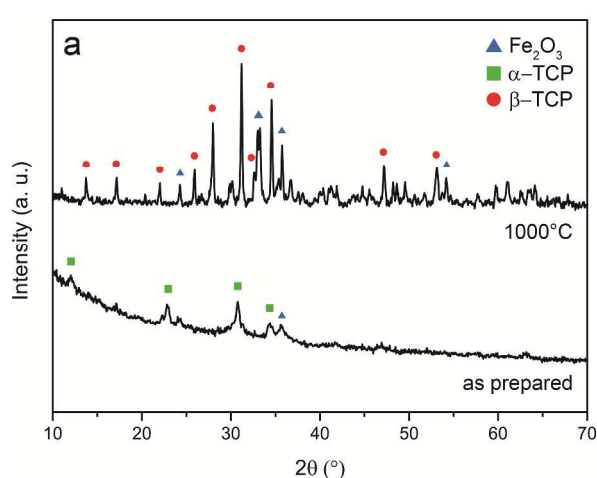
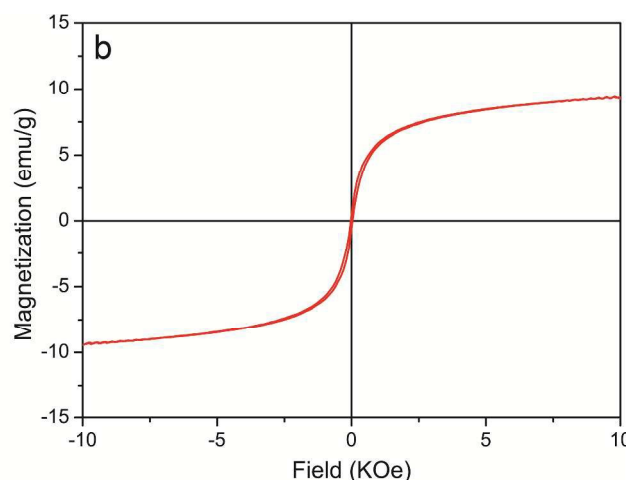


Fig. 4 (a) XRD pattern and (b) hysteresis loop of Fe_2O_3 @TCP nanoparticles.



calculated assuming spherical particles and using the overall density of the composite material (see Supplementary Information for density and size calculations). Transmission electron microscopy (TEM; Fig. 2 and Fig. S1) and scanning transmission electron microscopy (STEM; Fig. 3a) images supported the assumption of agglomerated spherically shaped nanoparticles. Energy-dispersive X-ray (EDX) mapping (Fig. 3b-e) of the particles showed spherical iron oxide nanoparticles embedded in the TCP matrix, suggesting a core/shell-like structure. The X-ray diffraction (XRD) pattern, shown in Fig. 4a, confirmed the presence of Fe_2O_3 and revealed the coexistence of amorphous and α -TCP. Iron oxide nanocrystallite size, calculated from the XRD pattern by means of the Scherrer formula, was estimated to be 10 nm. As expected, after heating the material to 1000°C, X-ray diffraction pattern showed peaks ascribed to β -TCP (Fig. 4a).²⁸ Vibrating sample magnetometry (VSM) data (Fig. 4b) revealed a saturation magnetization of 9.3 emu/g. Mean hydrodynamic particle diameter measured by X-ray disk centrifuge (XDC) was 121 nm, significantly larger than the calculated primary diameter, which can be explained by the formation of

aggregates. Full hydrodynamic size distribution is given in the Supplementary Information (Fig. S2). The average number of primary particles per aggregate was estimated to be 17 (Supplementary Information). A surface zeta potential of -14.8 mV was measured.

After characterizing the produced powder, we proved that the outer TCP surface allows for pDNA binding in the presence of CaCl_2 , as evidenced by Qubit fluorometric quantitation ($\sim 0.02 \mu\text{g}$ DNA per μg of nanoparticles, changing with plasmid size), gel electrophoresis (Fig. S3), and surface zeta potential data (-18.2 mV). Most probably Ca^{2+} ions mediate DNA-particles binding through electrostatic interactions.

Particle size and ability to bind pDNA were not changed after powder long term storage at room temperature (see Supplementary Information).

To demonstrate the applicability of the particles as transfection agents we used them to deliver a GFP encoding plasmid into HEK 293 cells. GFP expression demonstrated successful cell transfection. Experimental conditions were optimized to maximize the transfection rate of Fe_2O_3 @TCP particles while minimizing effects on cell proliferation. Best conditions were

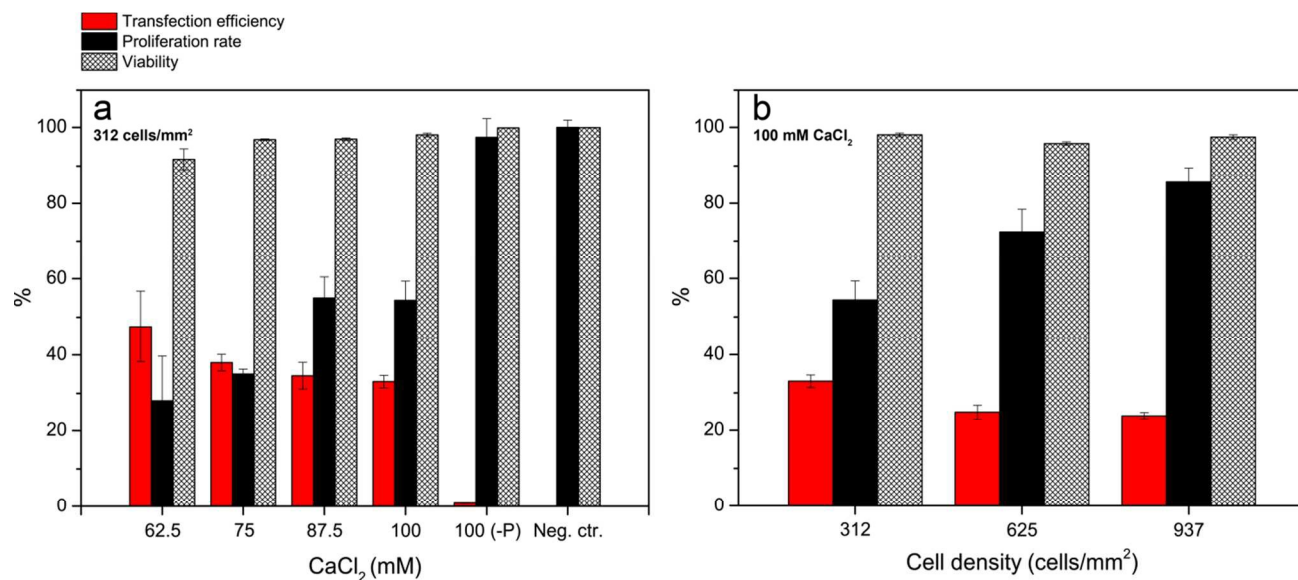


Fig. 5 Transfection efficiency, proliferation rate and viability in HEK 293 cells transfected with $\text{Fe}_2\text{O}_3@\text{TCP}$ while varying (a) CaCl_2 concentration (fixed cell density: 312 cells/ mm^2) or (b) cell seeding density (fixed CaCl_2 concentration: 100 mM). Samples incubated with naked DNA, CaCl_2 /saline buffer without particles (-P), and untreated samples (neg. ctr.) are shown for comparison.

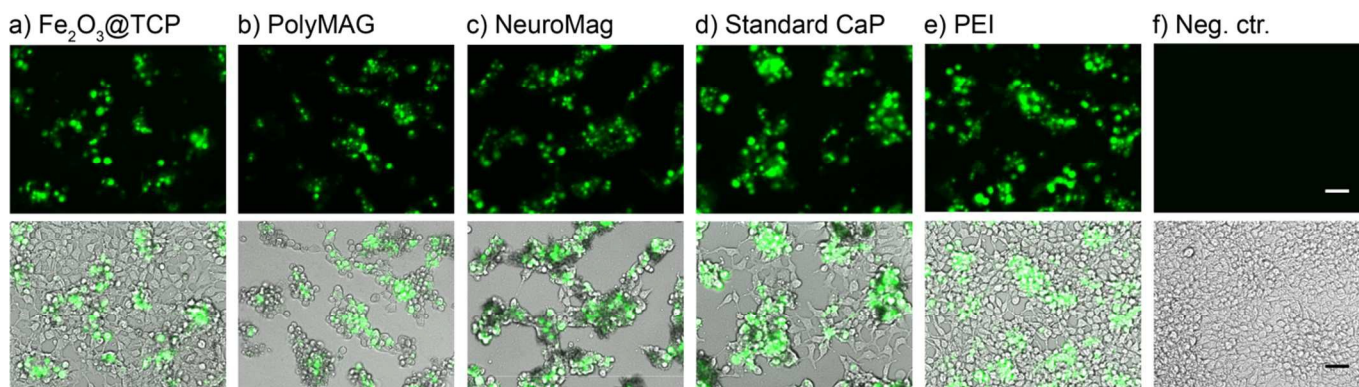


Fig. 6 GFP fluorescence microscopy (upper row) and merged fluorescence and bright field microscopy images (lower row) of HEK 293 transfected with $\text{Fe}_2\text{O}_3@\text{TCP}$ (a), with the commercial transfection agents PolyMAG (b) and NeuroMag (c), with standard CaP method (d) and with PEI (e). Untreated control is also shown (f). Images are representatives of $n = 3$ experiments. Scale bar: 50 μm .

found to be particle:DNA ratio 4:1 (4 μg particle per μg of DNA) and a cell density of 937 cells/ mm^2 . Cell viability throughout the experiments was in the range of 92-98%, not showing marked particle induced toxicity. Transfection efficiency in HEK 293 cells increased from ~33% to ~48% with decreasing CaCl_2 concentration (Fig. 5a), when cells were seeded at a density of 312 cells/ mm^2 . Conversely, proliferation increased with increasing CaCl_2 concentration. A loss in transfection was thought as acceptable in favour of an increase in cell proliferation rate, an indicator of cell health. Therefore, a CaCl_2 concentration in the range 87.5-100 mM was considered as optimal for transfection purposes. Notably, only a negligible number of transfected cells were observed in presence of CaCl_2 without particles. Cell viability in the negative controls (untreated) was always about 100% and, as expected, no GFP was detected. In Fig. 5b data resulting from cell transfection

with $\text{Fe}_2\text{O}_3@\text{TCP}$ and 100 mM CaCl_2 while varying starting cell density are shown. We observed less transfected cells and higher proliferation rate with increased cell density, less DNA-particle conjugates being available per cell. In optimal conditions (937 cells/ mm^2 , 100 mM CaCl_2), $\text{Fe}_2\text{O}_3@\text{TCP}$ were only marginally affecting cell growth, with a proliferation rate of ~86%. As illustrated in Fig. 6a, cells showed a normal, spread morphology.

After optimizing transfection with $\text{Fe}_2\text{O}_3@\text{TCP}$, we compared the technique to other existing transfection methods. Fluorescence microscopy micrographs and overlay images from fluorescence and bright field microscopy (Fig. 6) show the GFP expression in samples treated with $\text{Fe}_2\text{O}_3@\text{TCP}$ particles and with the other transfection agents. Transfection, proliferation and viability data are graphically represented in Fig. 7. One-way ANOVA statistical test was used to estimate global

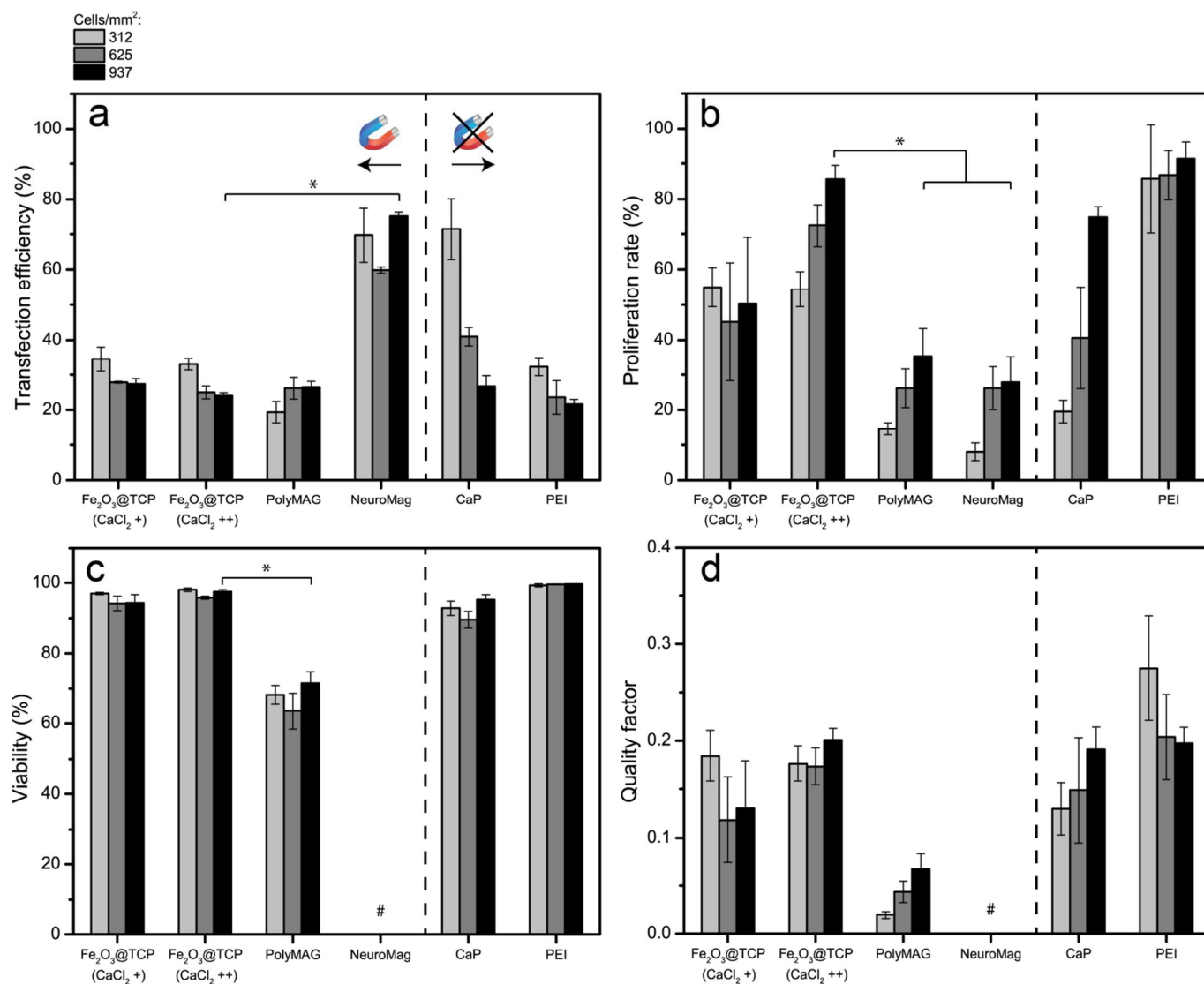


Fig. 7 (a) Transfection efficiency, (b) proliferation rate, (c) viability and (d) quality factor for HEK 293 cells at various cell seeding density after transfection with Fe₂O₃@TCP and 87.5 mM CaCl₂ (+) or 100 mM CaCl₂ (++) with PolyMAG, NeuroMag, standard CaP and PEI; # data missing due to NeuroMag fluorescence; * $p < 0.0001$ versus Fe₂O₃@TCP (CaCl₂ ++) at the same density (Bonferroni post test).

differences among the methods. Subsequently, Bonferroni *post hoc* test was applied for transfection, proliferation, and viability mean values comparison (0.05 significance level). Statistical analysis results are summarized in Table S2. With PolyMAG transfection efficiencies were comparable to results obtained with Fe₂O₃@TCP and 100 mM CaCl₂. Conversely, with NeuroMag we achieved significantly higher transfection rates (~60–75%) than with Fe₂O₃@TCP particles ($p < 0.001$ at all cell densities). CaP gave significantly better results than Fe₂O₃@TCP particles in term of transfection efficiency when cells were seeded at 312 and 625 cells/mm² ($p < 0.001$ in both cases), while results were comparable when starting cell density was 937 cells/mm². With PEI we obtained transfection rates not significantly different from those with Fe₂O₃@TCP and 100 mM CaCl₂.

Transfection efficiency is the key factor indicating how many

cells the plasmid was able to enter, but it can be an unfair parameter: if the method significantly affects cell proliferation and physiology, high efficiencies can be obtained since cells remain few in number and, thus, most of them result transfected. Even if not dead, those cells are possibly very unhealthy. Additionally, this translates in low density of transfectants (number of transfectants per surface unit), a disadvantage in many applications such as protein manufacturing. For this reasons we decided to include an additional parameter, *i.e.* cell proliferation, to rigorously judge how efficient a transfection agent is. An optimal transfection tool should provide simultaneously high transfection efficiency, proliferation rate and viability. The quality factor introduced, taking into account the three equally important variables, is therefore the most natural measure to properly evaluate the overall performance of the different methodologies. If just one

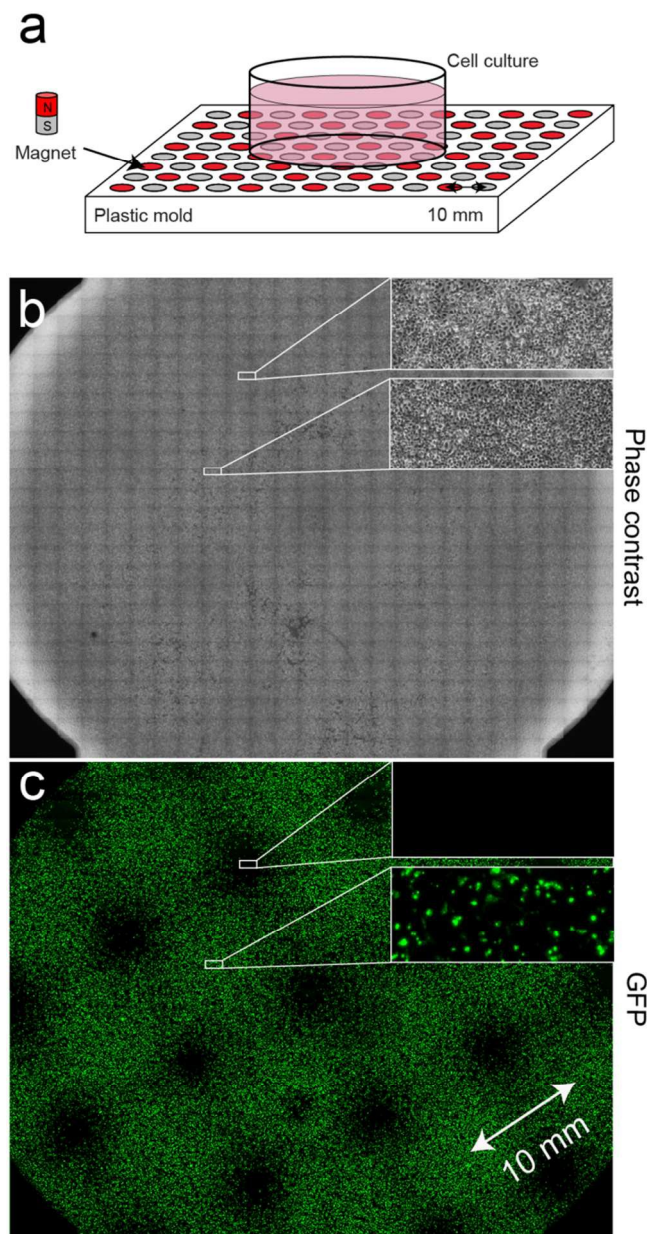


Fig. 8 (a) Scheme of the experimental set-up used: cells in a Petri dish are placed on a magnetic array, featuring permanent magnets in a plastic mold; (b) phase contrast image illustrating cells equally spread all over the Petri dish, with zoom on non-transfected cells and on transfected ones; (c) GFP fluorescence image proving that $\text{Fe}_2\text{O}_3@\text{TCP}$ magnetic particles allow localized control of gene expression in areas overlaying magnet positions and in between poles of opposite polarity, leaving not transfected spots between poles of same polarity; zoom on a green area and on a dark spot are also shown.

of the three variables is very small, the QF value is drastically affected.

As expected, PolyMAG and NeuroMag highly affected cell proliferation, which was significantly lower when compared to results obtained with $\text{Fe}_2\text{O}_3@\text{TCP}$ particles ($p < 0.001$ in all cases). Cells incubated with PolyMAG and NeuroMag were rounded, detached and clumped, a clear sign of induced damage (Fig. 6b and c). Viability of cells treated with PolyMAG was in the range of 64-72% as reported elsewhere,⁴¹ and therefore

significantly lower ($p < 0.0001$ at all cell densities) than in samples incubated with $\text{Fe}_2\text{O}_3@\text{TCP}$ particles. PolyMAG cytotoxicity was most likely associated to the presence of polycations.⁶ NeuroMag had most probably a similar toxic effect on cells, as judged from the atypical, round morphology. Unfortunately, we could not estimate cell viability in samples transfected with NeuroMag since particles showed a strong red fluorescence which did not allow to distinguish red-fluorescent dead cells stained with ethidium homodimer-1, and represents an obstacle for *in vitro* fluorescence microscopy investigations. With standard CaP precipitates, proliferation rate was strongly dependent on starting cell density and significantly lower (at 312 and 625 cells/ mm^2 , $p < 0.05$ in both cases) or comparable (937 cells/ mm^2) to that with $\text{Fe}_2\text{O}_3@\text{TCP}$ particles. Cells were considered generally healthy by morphological examination (Fig. 6d), with a viability of $\geq 90\%$ at each cell density. Surprisingly, PEI did not show toxic effects. Proliferation rates with PEI were significantly higher (at 312 cells/ mm^2 , $p < 0.01$) or comparable (at the other two cell densities) to those in samples transfected with $\text{Fe}_2\text{O}_3@\text{TCP}$ particles. The absence of cytotoxicity was possibly due to the low molecular weight of the PEI chosen, combined with the use of a not too high N:P ratio.⁴² Morphological inspection of cells transfected with PEI confirmed the healthy status of the cells. Cells were $\geq 99\%$ viable.

As the Figure 7 illustrates, QF was equally high for $\text{Fe}_2\text{O}_3@\text{TCP}$ particles, CaP and PEI, while Polymag had a significantly lower score. Therefore, taking into account all the analyzed factors, $\text{Fe}_2\text{O}_3@\text{TCP}$ particles perform better than PolyMAG, and are generally comparable to CaP and PEI, which are though non-magnetic and therefore cannot be magnetically targeted to a desired site.

Even though the application of a magnetic field gradient did not increase transfection efficiency of $\text{Fe}_2\text{O}_3@\text{TCP}$ particles (data not shown), it allowed to guide them by magnetic means and induce localized gene expression. We showed the possibility to achieve spatial control of transfection by creating the pattern illustrated in Fig. 8, where GFP expression is observed only in areas defined by the magnetic gradients applied. The magnetic array used to achieve such result is formed by cylindrical permanent magnets inserted into a plastic support in an alternating polarization manner from each adjacent permanent magnet (Fig. 8a). Due to this arrangement, highest field gradients are produced in the region above the magnet positions, where most of the particles are guided, producing the highest density of transfected cells (Fig. 8c). Lower magnetic gradients are present between poles of opposite polarity, where a lower density of transfected cells is observed. Transfectant density approximates zero in areas between poles of same polarity repulsing each other (Fig. 8c). Such a platform allowing site-specific transfection would be suitable for gene screening as well as for engineering of complex tissues *in vitro*.

Conclusions

In summary, we designed and produced for the first time Fe₂O₃@TCP nanoparticles by flame spray synthesis. The intrinsic non-toxicity of the components and the magnetic properties of the composite powder make it a promising candidate for magnetically guided nucleic acid delivery. The particles were successfully used to transfect HEK 293 cells, without compromising cell viability or inducing changes in cell morphology. Fe₂O₃@TCP nanoparticles were further compared to other transfection agents: two magnetic commercial options (PolyMAG and NeuroMag), standard CaP co-precipitates and PEI. Although highest transfection efficiencies were obtained with NeuroMag, Fe₂O₃@TCP nanoparticles did not have the negative influence on cell growth and morphology that both commercial magnetic transfection agents induced. Overall Fe₂O₃@TCP nanoparticle performance, considering together transfection efficiency, proliferation rate, and viability, were similar to that of CaP and PEI. An enhancement with respect to CaP and PEI was achieved thanks to the magnetic properties of the particles, which allowed spatially controlled transfection. These results suggest possible method applications for site-specific gene expression control in synthetic biology and regenerative medicine.

Acknowledgments

We thank ETH Zurich (Institute for Chemical and Bioengineering) and the EU-ITN network Mag(net)icFun (PITN-GA-2012-290248) for financial support, Hanspeter Hächler for magnetic hysteresis measurements, and Frank Krumeich for electronic microscopy and energy-dispersive X-ray spectroscopy.

Notes and references

^a Institute for Chemical and Bioengineering, Department of Chemistry and Applied Biosciences, ETH Zurich, 8093 Zurich, Switzerland

^b Department of Health Sciences and Technology, ETH Zurich, 8093 Zurich, Switzerland

^c Department of Preventive Dentistry, Periodontology, and Cariology, University of Zurich, Center for Dental Medicine, 8032 Zurich, Switzerland

*Corresponding author:

e-mail: robert.grass@chem.ethz.ch; phone: +41 44 633 63 34; fax: +41 44 633 10 83

Electronic Supplementary Information (ESI) available: particle characterization methods; TEM micrograph of Fe₂O₃@TCP nanoparticles; particle density calculation; primary particle size and number of particle per aggregate calculations; procedure for preparation and transformation of chemically competent E. coli; DNA binding assay; microscopy; live/dead assay and cell counting procedure; statistical analysis. See DOI: 10.1039/b000000x/

1. S. K. Tripathy, H. B. Black, E. Goldwasser and J. M. Leiden, *Nat Med*, 1996, **2**, 545.
2. W. T. Godbey, K. K. Wu and A. G. Mikos, *J Controlled Release* 1999, **60**, 149.
3. C. Y. M. Hsu and H. Uludag, *Nat Protoc*, 2012, **7**, 935.
4. Y. Hu, N. N. Zhao, B. R. Yu, F. S. Liu and F. J. Xu, *Nanoscale*, 2014, **6**, 7560.
5. N. Skandrani, A. Barras, D. Legrand, T. Gharbi, H. Boulahdour and R. Boukherroub, *Nanoscale*, 2014, **6**, 7379.
6. D. Fischer, Y. X. Li, B. Ahlemeyer, J. Kriegelstein and T. Kissel, *Biomaterials*, 2003, **24**, 1121.
7. F. Graham and A. Van der Eb, *Virology*, 1973, **52**, 456.
8. M. Wigler, S. Silverstein, L. S. Lee, A. Pellicer, Y. C. Cheng and R. Axel, *Cell*, 1977, **11**, 223.
9. M. Jordan, A. Schallhorn and F. M. Wurm, *Nucleic Acids Res*, 1996, **24**, 596.
10. S. V. Dorozhkin and M. Epple, *Angew Chem-Int Edit*, 2002, **41**, 3130.
11. D. Tadic and M. Epple, *Biomaterials*, 2004, **25**, 987.
12. F. Theiss, D. Apelt, B. A. Brand, A. Kutter, K. Zlinszky, M. Bohner, S. Matter, C. Frei, J. A. Auer and B. von Rechenberg, *Biomaterials*, 2005, **26**, 4383.
13. K. Rezwani, Q. Z. Chen, J. J. Blaker and A. R. Boccaccini, *Biomaterials*, 2006, **27**, 3413.
14. J. Hu, A. Kovtun, A. Tomaszewski, B. B. Singer, B. Seitz, M. Epple, K.-P. Steuhl, S. Ergün and T. A. Fuchsluger, *Acta Biomater*, 2012, **8**, 1156.
15. R. Z. LeGeros, *Chem Rev*, 2008, **108**, 4742.
16. M. Epple, V. V. Sokolova, I. Radtke and R. Heumann, *Biomaterials*, 2006, **27**, 3147.
17. F. Scherer, M. Anton, U. Schillinger, J. Henkel, C. Bergemann, A. Kruger, B. Gansbacher and C. Plank, *Gene Ther*, 2002, **9**, 102.
18. J. Dobson, *Gene Ther*, 2006, **13**, 283.
19. D. Ang, Q. V. Nguyen, S. Kayal, P. R. Preiser, R. S. Rawat and R. V. Ramanujan, *Acta Biomater*, 2011, **7**, 1319.
20. M. Isalan, M. I. Santori, C. Gonzalez and L. Serrano, *Nat Med*, 2005, **2**, 113.
21. T. Houchin-Ray, K. J. Whittlesey and L. D. Shea, *Mol Ther*, 2007, **15**, 705.
22. J. Hasty, D. McMillen and J. J. Collins, *Nat*, 2002, **420**, 224.
23. J. Ziauddin and D. M. Sabatini, *Nat*, 2001, **411**, 107.
24. C. C. Chen, Y. P. Lin, C. W. Wang, H. C. Tzeng, C. H. Wu, Y. C. Chen, C. P. Chen, L. C. Chen and Y. C. Wu, *J Am Chem Soc*, 2006, **128**, 3709.
25. W. W. Hu, Z. Wang, S. J. Hollister and P. H. Krebsbach, *Gene Ther*, 2007, **14**, 891.
26. M. I. Santori, C. Gonzalez, L. Serrano and M. Isalan, *Nat Protoc*, 2006, **1**, 526.
27. L. Madler, H. K. Kammler, R. Mueller and S. E. Pratsinis, *J Aerosol Sci*, 2002, **33**, 369.
28. S. Loher, W. J. Stark, M. Maciejewski, A. Baiker, S. E. Pratsinis, D. Reichardt, F. Maspero, F. Krumeich and D. Gunther, *Chem Mater*, 2005, **17**, 36.
29. C. M. Schumacher, I. K. Herrmann, S. B. Bubenhofer, S. Gschwind, A.-M. Hirt, B. Beck-Schimmer, D. Guenther and W. J. Stark, *Adv Funct Mater*, 2013, **23**, 4888.
30. R. Weissleder, D. D. Stark, B. L. Engelstad, B. R. Bacon, C. C. Compton, D. L. White, P. Jacobs and J. Lewis, *Am J Roentgenol*, 1989, **152**, 167.
31. A. K. Gupta and M. Gupta, *Biomaterials*, 2005, **26**, 3995.
32. M. K. Yu, Y. Y. Jeong, J. Park, S. Park, J. W. Kim, J. J. Min, K. Kim and S. Jon, *Angew Chem-Int Edit*, 2008, **47**, 5362.
33. T. K. Jain, M. K. Reddy, M. A. Morales, D. L. Leslie-Pelecky and V. Labhasetwar, *Mol. Pharm.*, 2008, **5**, 316.
34. Y. Wu, W. Jiang, X. Wen, B. He, X. Zeng, G. Wang and Z. Gu, *Biomed Mater* 2010, **5**.
35. Z. Tang, Y. Zhou, H. Sun, D. Li and S. Zhou, *Eur J Pharm Biopharm*, 2014, **87**, 90.
36. R. N. Grass, T. F. Albrecht, F. Krumeich and W. J. Stark, *J Mater Chem*, 2007, **17**, 1485.
37. A. Teleki, M. Suter, P. R. Kidambi, O. Ergeneman, F. Krumeich, B. J. Nelson and S. E. Pratsinis, *Chem Mat*, 2009, **21**, 2094.

Journal Name

38. W. J. Stark, A. Baiker and S. E. Pratsinis, *Part Part Syst Char*, 2002, **19**, 306.
39. N. Osterwalder, C. Capello, K. Hungerbuhler and W. J. Stark, *J Nanopart Res*, 2006, **8**, 1.
40. N. Link, T. J. Brunner, I. A. J. Dreesen, W. J. Stark and M. Fussenegger, *Biotechnol Bioeng* 2007, **98**, 1083.
41. S.-J. Huang, J.-H. Ke, G.-J. Chen and L.-F. Wang, *J Mater Chem B*, 2013, **1**, 5916.
42. U. Lungwitz, M. Breunig, T. Blunk and A. Gopferich, *Eur J Pharm Biopharm*, 2005, **60**, 247.